Pis'ma v ZhETF, vol. 102, iss. 2, pp. 125 – 129

Anisotropic flat bands on the surface of multilayer graphenelike lattice

A. A. Zyuzin[+*1)], V. A. Zyuzin[×]

[+]Department of Physics, University of Basel, CH-4056 Basel, Switzerland

[*]Ioffe Physico-Technical Institute of the RAS, 194021 St. Petersburg, Russia

[×]Department of Physics, University of Florida, FL 32611-8440 Gainesville, USA

Submitted 15 June 2015

The fermionic energy spectrum on the surface of the multilayer honeycomb lattice with rhombohedral stacking has topologically protected flat bands. It is shown that topological phase transition occurs in the anisotropic multilayer graphene-like structure with strongly anisotropic intra-layer coupling, at which two flat bands with opposite chirality merge into one and split, opening up a gap in the energy spectrum, depending on the anisotropy of the intralayer hopping. The dispersion of the flat bands of the multilayer is anisotropic and the density of states is more singular in the vicinity of the transition.

DOI: 10.7868/S0370274X15140106

I. Introduction. It is well known that topological surface states can exist in the absence of the gap in the bulk of the structure. The energy spectrum in the bulk of the three dimensional topological semimetal might host a nodal line formed by zeroes in momentum space. Projection of this nodal line on the surface Brillouin zone (BZ) of the semimetal forms the flat band for electrons in the vicinity to the surface. The stability of the flat band to the interactions and disorder is protected by the topological invariant corresponding to the nodal line, the so called bulk-edge correspondence [1–3].

There is a number of theoretically proposed nodal systems that might host flat band in the energy spectrum on the surface such as topological insulator multilayers [4, 5], multilayer graphene-like structures [6–8], nodal superconductors [9–12]. Due to very singular density of states of the flat band, graphene-like layered systems were proposed to give rise to the high-temperature surface superconductivity [11, 12]. Many more examples of gapless topological systems that support nontrivial surface states (Fermi arcs in three dimensional Weyl semimetals [13, 14, 15, 16], flat bands at the zig-zag edge of graphene [17]) can be found in the review [3].

Here we consider the tight binding model of electrons on the multilayer honeycomb lattice with the rhombohedral stacking of layers, taking into account the anisotropic hopping between the nearest-neighbour sites in each layer, see Fig. 1a.

We start our discussion from noting that a single layer honeycomb lattice undergoes a quantum phase transition, driven by the anisotropy of the hopping elements between nearest neighbor sites, from an insulating to a semimetallic state [18–22]. Electrons on the honeycomb lattice have Dirac spectrum at two inequivalent corners of the Brillouin zone. Each Dirac point can be characterized by a topological invariant: the wind-

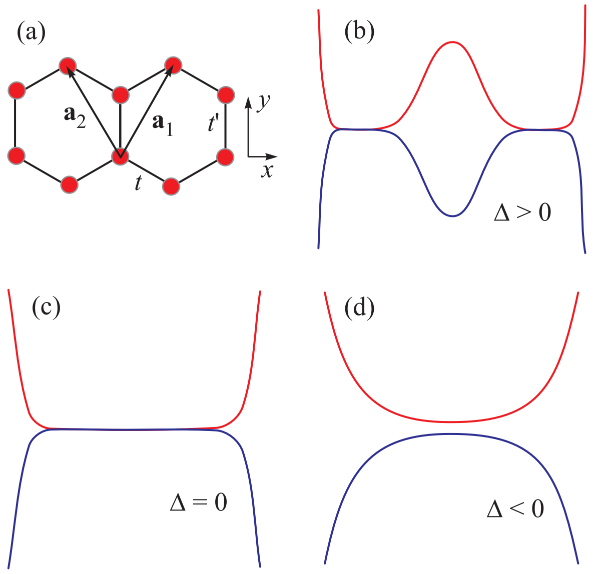

Fig. 1. (a) – Honeycomb lattice with anisotropic hopping elements. (b) – $k_y = 0$ section of the surface band dispersion of the multilayer honeycomb lattice, plotted at different values of the hopping element anisotropy $\Delta = 2t - t'$. Band structure for $\Delta > 0$. Two flat bands are separated along the x direction. (c) – Critical point $\Delta = 0$, where two flat bands merge into one. (d) – Band structure in the gapped phase $\Delta < 0$

[1)] e-mail: a.zyuzin@unibas.ch

ing number around any surface in momentum space, enclosing the point [1, 2, 23]. Strong anisotropy of the hopping elements breaks the twofold valley degeneracy corresponding to the two Dirac points. The pair of Dirac points can be annihilated by merging these points together at special values of the hopping elements. The detailed review of the properties of the anisotropic graphenelike systems can be found in [17, 24].

The multilayer with rhombohedral stacking of honeycomb lattice layers possesses interesting electronic properties. The energy spectrum of electrons on the outer surfaces of such multilayer has a form of the flat band, while the bulk energy spectrum possesses spiral nodal lines [8, 5, 17]. Projection of two nodal spiral on the outer edges of the multilayer defines the boundaries of the of flat bands at two inequivalent corners of the BZ of honeycomb lattice. The opposite winding of two nodal lines in momentum space reflects in the opposite chiralities of the corresponding flat bands on the surface.

We show that the in-plane anisotropic hopping at fixed interlayer hopping transforms two nodal spirals into a single nodal loop. Strong in-plane anisotropy squeezes the nodal loop into a single point and then gaps out the spectrum. We show that due to the bulk-surface correspondence there occurs a quantum phase transition on the surface of the anisotropic honeycomb multilayer structure, at which two flat bands merge into one and then split opening up a gap in the surface spectrum, Fig. 1.

II. Single layer. Here for the readers convenience we first review the details of the band structure and describe the phase transition in the single anisotropic layer and then make generalization to the multilayered structure.

The tight binding approximation for the electrons on the honeycomb lattice is taken within the minimal model of the nearest-neighbour hopping between the sites. The nearest-neighbour hopping element along y-axis is defined by t' and assumed to be different from two other nearest-neighbour matrix elements, which are defined by t, see Fig. 1a. Parameters t and t' are assumed to be real and positive constants.

The triangular lattice with two atoms per unit cell is defined by lattice vectors, which can be written as $\mathbf{a}_1 = a(\sqrt{3}\mathbf{e}_x+3\mathbf{e}_y)/2$ and $\mathbf{a}_2 = a(-\sqrt{3}\mathbf{e}_x+3\mathbf{e}_y)/2$, where a is the distance between the nearest-neighbour sites and $\mathbf{e}_i$, $i = x, y, z$ are the basis vectors. The three vectors that connect nearest-neighbour sites on the lattice are defined as $\boldsymbol{\delta}_1 = a(\sqrt{3}\mathbf{e}_x+\mathbf{e}_y)/2$, $\boldsymbol{\delta}_2 = a(-\sqrt{3}\mathbf{e}_x+\mathbf{e}_y)/2$, and $\boldsymbol{\delta}_3 = -a\mathbf{e}_y$. The Hamiltonian of the monolayer honeycomb lattice with anisotropic hopping is given by:

$$\mathcal{H} = -\frac{t}{2}\sum_{\sigma,\mathbf{k}} \Psi^\dagger_{\sigma,\mathbf{k}}[\gamma^*_{\mathbf{k}}\sigma_+ + \gamma_{\mathbf{k}}\sigma_-]\Psi_{\sigma,\mathbf{k}}, \tag{1}$$

where $\Psi_{\sigma,\mathbf{k}} = (a_{\sigma,\mathbf{k}}, b_{\sigma,\mathbf{k}})^{\mathrm{T}}$, $a_{\sigma,\mathbf{k}}$ and $b_{\sigma,\mathbf{k}}$ are the annihilation operators of electron with spin projection $\sigma =\uparrow,\downarrow$ on two sublattices of the honeycomb lattice; $\sigma_\pm = \sigma_x \pm i\sigma_y$, where σ_j, $j = (x, y, z)$, is the Pauli matrix acting on the sublattice pseudospin degree of freedom. Taking into account only nearest-neighbour hopping, one obtains:

$$\gamma_{\mathbf{k}} = [t'/t + 2\cos(\sqrt{3}ak_x/2)e^{i\cdot 3ak_y/2}]e^{-iak_y}. \tag{2}$$

Diagonalizing the Hamiltonian (1), one obtains energy spectrum of the monolayer:

$$E_{\mathbf{k}\pm} = \pm t|\gamma_{\mathbf{k}}|. \tag{3}$$

The anisotropy of tunnelling matrix elements shifts the positions of two Dirac points from the corners of the BZ, defined by $\left(\pm\frac{2\pi}{3\sqrt{3}a}, \frac{2\pi}{3a}\right)$. The positions of two shifted Dirac points can be found by solving equation $\gamma_{\mathbf{k}} = 0$:

$$k_{x\mathrm{D}\pm} = \pm\frac{2}{\sqrt{3}a}\arccos\left(\frac{t'}{2t}\right), \quad k_{y\mathrm{D}} = \frac{2\pi}{3a}, \tag{4}$$

where $\pm$ sign corresponds to two inequivalent Dirac points. As long as $t' < 2t$, two Dirac points are separated in momentum space. At critical value of hopping parameters $t' = 2t$, two Dirac points merge into one point at position:

$$k_{xM} = 0, \quad k_{yM} = \frac{2\pi}{3a}. \tag{5}$$

The further increase of the anisotropy opens up a gap in the energy spectrum. To see this explicitly [24], the energy spectrum can be expanded ($k_x \to k'_x = k_{xM} + k_x$, $k_y \to k'_y = k_{yM} + k_y$) in the vicinity of the point (k_{xM}, k_{yM}):

$$E^2_{\mathbf{k}} = \left(\frac{k_x^2}{2m} - \Delta\right)^2 + c^2k_y^2, \tag{6}$$

where $m = 2/3ta^2$ is the effective mass, $c = 3ta$ is the Fermi velocity along y direction, and $\Delta = 2t - t'$. Note that for $\Delta > 0$ the energy spectrum of the monolayer has two Dirac points at $k_{x\pm} = \pm\sqrt{2m\Delta}$, $k_y = 0$, while for $\Delta < 0$ the spectrum is gapped. The quantum phase transition from semimetal to insulator state of the lattice takes place when $\Delta = 0$ [18–20, 24]. In the vicinity of the transition point on the semimetal side, the band dispersion is anisotropic. It is quadratic along the x direction, but remains linear in the y direction.

III. Multi-layered structure. Multi-layer structure build from two-dimensional atomic layers with

Dirac points in the band spectrum of each layer might host a topological flat band on its surface [7, 8].

Let us show how these flat bands are realized by considering the N-layer rhombohedrally stacked honeycomb lattice with anisotropic hopping within each layer. We take into account only nearest-neighbour hopping between different layers. The low energy fermionic spectrum on the surface of the N-layer isotropic honeycomb lattice has the form of $E^2 \propto |\mathbf{k}|^{2N}$, which approaches a flat band as the number of layers increases, $N \to \infty$, see review [17]. The Hamiltonian of the rhombohedrally stacked N-layer honeycomb lattice can be written as

$$\mathcal{H}_{\rm ML} = -\frac{1}{2}\sum_{\sigma,\mathbf{k}}\sum_{j>0}^{N}\Psi^{\dagger}_{\sigma,\mathbf{k},i}\Big[(t\gamma^{*}_{\mathbf{k}}\delta_{i,j} + g\delta_{i-1,j})\sigma_{+} + + (t\gamma_{\mathbf{k}}\delta_{i,j} + g\delta_{i+1,j})\sigma_{-}\Big]\Psi_{\sigma,\mathbf{k},j}. \tag{7}$$

Here g defines the nearest-neighbour hopping matrix element between the layers, the indices i, j label distinct honeycomb layers, and $\Psi_{\sigma,\mathbf{k},i} = (a_{\sigma,\mathbf{k},i}, b_{\sigma,\mathbf{k},i})^{\rm T}$ is the electron annihilation operator on i-th lattice.

Diagonalizing Eq. (7) in the limit of infinite number of layers, $N \to \infty$, the effective Hamiltonian in momentum space is given by $\mathcal{H}_{\rm ML} = \frac{1}{2}\sum_{\sigma,\mathbf{k},\mathrm{k}_z}\Psi^{\dagger}_{\sigma,\mathbf{k},\mathrm{k}_z}H(\mathbf{k},\mathrm{k}_z)\Psi_{\sigma,\mathbf{k},\mathrm{k}_z}$, where

$$H(\mathbf{k},k_z) = -(t\gamma^{*}_{\mathbf{k}} + ge^{-ik_zd})\sigma_{+} - (t\gamma_{\mathbf{k}} + ge^{ik_zd})\sigma_{-}, \tag{8}$$

and d is the distance between the layers. One has the following band dispersion of the bulk system:

$$E^2_{\mathbf{k},\mathrm{k}_z} = \Big[t'\cos(ak_y) + 2t\cos(\sqrt{3}ak_x/2)\cos(ak_y/2) + + |g|\cos(k_zd)\Big]^2 + \Big[-t'\sin(ak_y) + + 2t\cos(\sqrt{3}ak_x/2)\sin(ak_y/2) + |g|\sin(k_zd)\Big]^2. \tag{9}$$

The energy spectrum of the bulk system has nodal spirals or loops depending on hopping parameters. Projection of these bulk nodal structures on the constant surface $k_z = $ const defines the region of the flat band on the surface in momentum space [8]:

$$t'^2 + 4tt'\cos(\sqrt{3}ak_x/2)\cos(3ak_y/2) + + 4t^2\cos(\sqrt{3}ak_x/2)^2 \leqslant |g|^2. \tag{10}$$

Each nodal spiral can be characterized by a topological invariant: the winding number around any surface in momentum space enclosing the nodal line [8, 22, 25, 26]. The winding numbers are equal to unity by magnitude and have opposite signs for the two nodal spirals.

The surface states of the multilayer graphene in the absence of the in-plane deformation $t' = t$ were studied in [8]. Similar surface states appear in the Shokley model of the three dimensional topological insulator on the diamond lattice [5]. In particular, it was shown [5] that special value of parameters $|g| = t$ marks the transition point between the nodal spiral phase $|g| < t$ and nodal loop phase $3t > |g| > t$ of the multilayer. Spiral phase has even number of nodal lines in the bulk spectrum. Nodal spirals are periodic in momentum k_z and wind around the points, given by expression (4). The spirals at two inequivalent points (4) in the BZ have opposite winding numbers. In the limit of strong interlayer tunnelling spirals intersect with each other forming odd number of nodal loops in the momentum space [5].

Here we consider the anisotropy of the intralayer hopping elements in the limit of weak interlayer coupling, when $t' > |g|$ and $t > |g|$, keeping the interlayer hopping element to be fixed.

In the vicinity of the merging point (5) we obtain the bulk energy spectrum in the form:

$$E^2_{\mathbf{k},\mathrm{k}_z} = \left[\frac{k_x^2}{2m} - \Delta + |g|\cos(k_zd)\right]^2 + + [ck_y - |g|\sin(k_zd)]^2. \tag{11}$$

The zeroes of the spectrum are defined by equations:

$$\frac{k_x^2}{2m} = \Delta - |g|\cos(k_zd), \quad ck_y = |g|\sin(k_zd). \tag{12}$$

The region of the surface states given by Eq. (10), in the vicinity of the point (5), is defined by the inequality:

$$c^2k_y^2 + (k_x^2/2m - \Delta)^2 \leqslant |g|^2. \tag{13}$$

At $\Delta > |g|$ two flat bands with opposite chirality do not overlap with each other in momentum space (Figs. 1b and 2). This is the nodal spiral phase in which spirals in momentum space do not intersect each other.

One observes a phase transition at $\Delta = |g|$ when two flat bands touch at one point with coordinates $k_x = 0$, $k_y = 0$ (Fig. 3). At this transition two nodal spirals touch each other at two points with coordinates $k_x = 0$, $k_y = 0$, $k_z = (0, 2\pi)$, forming a nodal loop.

With the further increase of the in-plane anisotropy $|g| > \Delta > 0$, the areas of two flat bands partially overlap reaching the full overlap at $\Delta = 0$. At this point flat band are doubly degenerate (Fig. 1c).

Energy gap opens up in the spectrum of the surface states when Δ becomes negative (Fig. 1d). The boundary of the surface states as well as the nodal loop

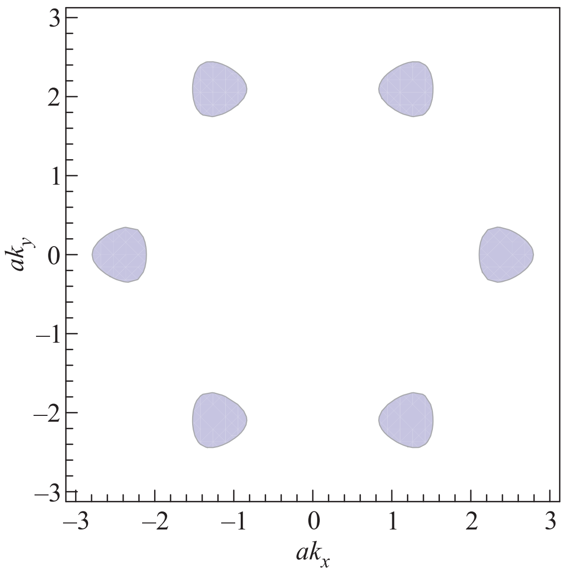

Fig. 2. Filled areas are projection of the nodal spirals to the $k_z = 0$ plane for parameters $t' = t$ and $g = 0.5t$. Projections form flat bands on the surface of the multilayer

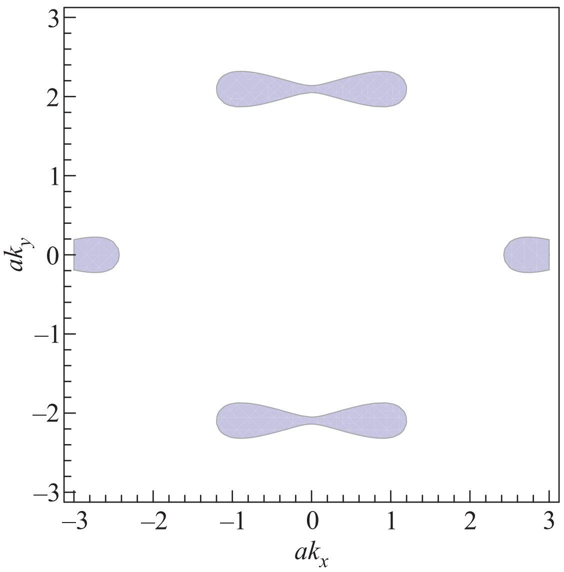

Fig. 3. Filled areas are projection of the nodal spirals to the $k_z = 0$ plane for parameters $t' = 1.5t$ and $g = 0.51t$. Flat bands start to overlap in momentum space with increase of the in-plane anisotropy

squeezes into a single point $k_x = 0$, $k_y = 0$, $k_z = \pi$ as $\Delta \to -|g|$. For $-|g| > \Delta$ Eq. (10) has no solutions.

The low energy band dispersion of the surface states of the N- layer honeycomb lattice in the limit $|g| \gg |t\gamma_{\mathbf{k}}|$ takes the form

$$E_{\mathbf{k}\pm} = \pm|g| \left(|t\gamma_{\mathbf{k}}|/|g|\right)^N . \tag{14}$$

Again, expanding the energy spectrum in the vicinity of merging point given by expression (5) one results with

$$E_{\mathbf{k}\pm} = \pm|g|^{1-N}[(k_x^2/2m - \Delta)^2 + c^2k_y^2]^{N/2}. \tag{15}$$

Two flat bands merge into one and open a gap as anisotropy parameter Δ changes sign to negative. In the vicinity of the phase transition the energy spectrum of the flat band is anisotropic. It has power law $2N$ dependence in the x direction and power law N dependence in the y direction.

Now we consider the density of states for the limit when two flat bands are separated in momentum space and for the insulating case. The density of states per spin is given as

$$\nu(\omega) = \int \frac{d^2k}{(2\pi)^2}\delta(\omega - E_{\mathbf{k}+}). \tag{16}$$

It is instructive to define a dimensionless parameter

$$z_\omega \equiv \left(|g|/\omega\right)^{1/N} \Delta/|g|. \tag{17}$$

If this parameter satisfies the inequality $|z_\omega| < 1$, then the density of states in the insulating state $\Delta < 0$ as well as in the gapless state $\Delta > 0$ has the following form

$$\nu(\omega) = \frac{\sqrt{2}\nu_0}{N} K\left(\frac{\sqrt{1+z_\omega}}{\sqrt{2}}\right)\left(\frac{|g|}{\omega}\right)^{1-3/2N}, \tag{18}$$

where $K(z)$ is the complete Elliptic integral of the first kind and $\nu_0 = \sqrt{2m|g|}/2\pi^2 c$. The density of states vanishes ($\nu(\omega) = 0$) in the insulating state for energies inside the gap at $z_\omega < -1$, while for $\Delta > 0$ and $z_\omega > 1$ one has

$$\nu(\omega) = \frac{2\nu_0}{N\sqrt{1+z_\omega}} K\left(\frac{\sqrt{2}}{\sqrt{1+z_\omega}}\right)\left(\frac{|g|}{\omega}\right)^{1-3/2N}. \tag{19}$$

The density of states diverges logarithmically at $z_\omega = 1$ and exhibits jump at $z_\omega = -1$. At large number of layers ($N \gg 1$) the density of states is inversely proportional to the energy and the number of layers $\nu(\omega) \propto |g|/N\omega$. The density of states on the surface of the multilayer becomes very singular as the number of layers increases. To compare, the density of states on the surface of the multilayer honeycomb lattice with isotropic intralayer hopping is less singular than in the anisotropic case and proportional $\nu(\omega) \sim (|g|/\omega)^{1-2/N}$.

IV. Conclusions. To conclude, we have studied the energy spectrum of the surface states of multilayer honeycomb lattice with rhombohedral stacking of layers as a function of anisotropy of the intralayer hopping elements. We have shown that the surface flat bands undergo a phase transition at critical value of the anisotropy, at which two flat bands with opposite chirality merge into one and then split opening the energy gap in the spectrum of the surface states, see Fig. 1 for details.

A promising system for the experimental feasibility of proposed surface states is the optical lattice [27–29]. Creating, moving and merging Dirac points was already experimentally demonstrated in a tunable honeycomb optical lattice [29].

It is theoretically established the the flat band might give rise to high temperature surface superconductivity, [11, 12]. We note that the deformation strongly enhances the singularity of the flat band DOS which might increase the transition temperature of the surface superconductivity.

We acknowledge useful discussions with A.A. Burkov, S. Pershoguba, L. Trifunovich, and A.Yu. Zyuzin. A.A.Z. acknowledges support from the Swiss NF and NCCR QSIT. V.A.Z. acknowledges support from the National Science Foundation via grant NSF DMR-1308972.

1. G. E. Volovik, *The Universe in a Helium Droplet*, Clarendon Press, Oxford (2003).
2. G. E. Volovik, Lect. Not. Phys. **718**, 31 (2007).
3. T. T. Heikkila, N. B. Kopnin, and G. E. Volovik, Pisma v ZhETF **94**, 252 (2011).
4. A. A. Burkov, M. D. Hook, and L. Balents, Phys. Rev. B **84**, 235126 (2011).
5. S. S. Pershoguba and V. M. Yakovenko, Phys. Rev. B **86**, 075304 (2012).
6. F. Guinea, A. H. Castro Neto, and N. M. R. Peres, Phys. Rev. B **73**, 245426 (2006).
7. T. T. Heikkila and G. E. Volovik, JETP Lett. **92**, 681 (2010).
8. T. Heikkila and G. E. Volovik, JETP Lett. **93**, 59 (2011).
9. S. Ryu and Y. Hatsugai, Phys. Rev. Lett. **89**, 077002 (2002).
10. A. P. Schnyder and S. Rue, Phys. Rev. B. **84**, 060504 (2011).
11. N. B. Kopnin, T. T. Heikkila, and G. E. Volovik, Phys. Rev. B **83**, 220503 (2011).
12. N. B. Kopnin, Pisma v ZhETF **94**, 81 (2011).
13. X. Wan, A. M. Turner, A. Vishwanath, and S. Y. Savrasov, Phys. Rev. B **83**, 205101 (2011).
14. L. Balents, Physics **4**, 36 (2011).
15. K. Y. Yang, Y. M. Lu, and Y. Ran, Phys. Rev. B **84**, 075129 (2011).
16. A. A. Burkov and L. Balents, Phys. Rev. Lett. **107**, 127205 (2011).
17. A. H. Castro Neto, F. Guinea, N. M. R. Peres, K. S. Novoselov, and A. K. Geim, Rev. Mod. Phys. **81**, 109 (2009).
18. P. Dietl, F. Piechon, and G. Montambaux, Phys. Rev. Lett **100**, 236405 (2008).
19. V. Pardo and W. E. Pickett, Phys. Rev. Lett. **102**, 166803 (2009).
20. K. Esaki, M. Sato, M. Kohmoto, and B. I. Halperin, Phys. Rev. B **80**, 125405 (2009).
21. G. Montambaux, F. Piechon, J. N. Fuchs, and M. O. Goerbig, Phys. Rev. B **80**, 153412 (2009).
22. G. Montambaux, F. Piechon, J. N. Fuchs, and M. O. Goerbig, Eur. Phys. J. B **72**, 509 (2009).
23. F. R. Klinkhamer and G. E. Volovik, Int. J. Mod. Phys. A **20**, 2795 (2005).
24. M. O. Goerbig, Rev. Mod. Phys **83** 1193 (2011).
25. J. L. Manes, F. Guinea, and M. A. H. Vozmediano, Phys. Rev. B **75**, 155424 (2007).
26. B. Beri, Phys. Rev. B **81**, 134515 (2010).
27. K. L. Lee, B. Gremaud, R. Han, B. G. Englert, and C. Miniatura, Phys. Rev. A **80**, 043411 (2009).
28. L. Mazza, A. Bermudez, N. Goldman, M. Rizzi, M. A. Martin-Delgado, and M. Lewenstein, New J. Phys. **14**, 015007 (2012).
29. L. Tarruell, D. Greif, T. Uehlinger, G. Jotzu, and T. Esslinger, Nature **483**, 302 (2012).